

Direct Observation of Long Electron-Hole Diffusion Distance beyond 1 Micrometer in $\text{CH}_3\text{NH}_3\text{PbI}_3$ Perovskite Thin Film

Yu Li,^{†,§} Weibo Yan,^{‡,§} Yunlong Li,[‡] Wei Wang,[†] Zuqiang Bian,^{,‡} Lixin Xiao,[†] Shufeng Wang,^{*,†} Qihuang Gong[†]*

[†]Institute of Modern Optics & State Key Laboratory for Artificial Microstructure and Mesoscopic Physics, School of Physics, Peking University, Beijing 100871, China.

[‡]State Key Laboratory of Rare Earth Materials Chemistry and Applications, College of Chemistry and Molecular Engineering, Peking University, Beijing, 100871, China

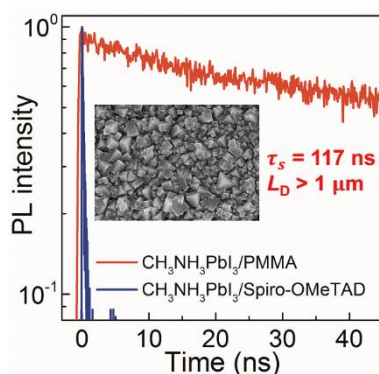
AUTHOR INFORMATION

Corresponding Authors

*Email: wangsf@pku.edu.cn; *Email: bianzq@pku.edu.cn

ABSTRACT: In high performance perovskite based on $\text{CH}_3\text{NH}_3\text{PbI}_3$, the formerly reported short charge diffusion distance is a confliction to thick working layer in solar cell devices. We carried out a study on charge diffusion in spin-coated $\text{CH}_3\text{NH}_3\text{PbI}_3$ perovskite thin film by transient fluorescent spectroscopy. A thickness-dependent fluorescent lifetime was found. This effect correlates to the defects at crystal grain boundaries. By coating the film with electron or hole transfer layer, [6,6]-phenyl-C₆₁-butyric acid methyl ester (PCBM) or 2,2',7,7'-tetrakis(N,N-di-p-methoxyphenylamine)-9,9'-spirobifluorene (Spiro-OMeTAD) respectively, we observed the charge transfer directly through the fluorescent decay. One-dimensional diffusion model was applied to obtain long charge diffusion distances, which is $\sim 1.3 \mu\text{m}$ for electrons and $\sim 5.2 \mu\text{m}$ for holes. This study gives direct support to the high performance of perovskite solar cells.

TOC GRAPHICS



KEYWORDS. perovskite; time-resolved photoluminescence; charge diffusion; photovoltaic; solar cell

Substantial attention has been drawn to the inorganic-organic perovskite-based solar cells, which currently achieve a certified high light conversion efficiency of 20.1%.¹ The combination of several excellent optoelectronic properties, such as very low exciton binding energy,^{2,3} highly mobile charge carriers,⁴⁻⁶ and efficient charge transportation to selective contact layers,^{3,5,7,8} makes perovskite remarkable materials for photovoltaic devices and “a new avenue of research”.⁹ As a fundamental issue, the carrier diffusion in perovskite is a major factor affecting the design and performance of the devices. However, this topic is still under debate at moment. It was shown that the charge diffusion distance in tri-iodine perovskite, $\text{CH}_3\text{NH}_3\text{PbI}_3$, is ~ 100 nm, studied by transient fluorescent spectroscopy.^{10,11} On the other hand, many high efficient perovskite solar cells based on $\text{CH}_3\text{NH}_3\text{PbI}_3$ were made with perovskite layers thicker than this distance.¹²⁻¹⁴ It is also investigated by impedance spectroscopy and electron beam-induced current (EBIC) method, which hint a much longer charge transfer distance within perovskite layer.^{15,16} A study on single crystal even give an extremely long diffusion length above $175\text{ }\mu\text{m}$.¹⁷ In addition, the diffusing balance between electrons and holes is not clear either. It was regarded that this balance is well maintained, while some reports say that the diffusion of holes are more/less efficient than electrons.^{16,18}

Beside the diffusion issue, some experimental observations are also in conflict. E.g. the fluorescent lifetime of the $\text{CH}_3\text{NH}_3\text{PbI}_3$ are dramatically varied in reports. In Xing’s report, the lifetime is 4.5 ns,¹⁰ while in Stranks’ report, it is 9.6 ns.¹¹ Some other experiments show that the lifetime for $\text{CH}_3\text{NH}_3\text{PbI}_3$ should be much longer than that. In reports by Yamada, the lifetime under low excitation light intensity can be 140 ns.¹⁹ In single crystal, it is even longer than $100\text{ }\mu\text{s}$ under low excitation intensity.¹⁷ This is an important parameter when calculate the charge diffusion

distance by one-dimensional diffusion model.^{10,11} It seems that all these conflicts need a better explanation.

To clarify these conflicts, we performed a study of directly observing the charge transfer in perovskite with various thicknesses and with an electron/hole transfer layer by means of time-resolved transient fluorescence. It shows here, that the charge diffusion in $\text{CH}_3\text{NH}_3\text{PbI}_3$ is of distance at micrometer scale, which obviously longer than film thickness. The study also explains why former studies provide short diffusion lengths. Also we show an unbalanced electron-hole charge transport ability within perovskite thin film.

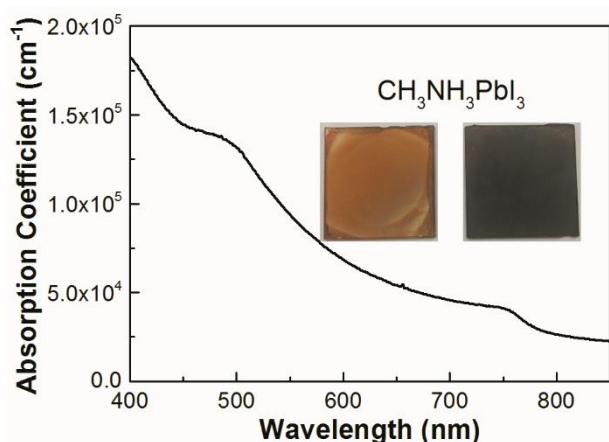


Figure 1. Absorption coefficient towards wavelength for $\text{CH}_3\text{NH}_3\text{PbI}_3$ thin film prepared via a two-step deposition method. Insets are the top view photos of perovskite samples of a thin (yellow brown, left) and a thick (dark brown, right) one on glass substrates.

All perovskite films discussed below were prepared by a two-step dipping procedure (see details in the Supporting Information (SI)) similar to a report and our study recently^{20,21} on flat glass substrates. Figure 1 shows the absorption coefficient of $\text{CH}_3\text{NH}_3\text{PbI}_3$ derived from the absorption spectrum according to Equation S3 in the SI. This spectrum, which is in line with former reports,

covers the entire UV and visible range up to 760 nm.^{10,22} At 517 nm (the wavelength of pump light), a coefficient of 1.2×10^5 cm⁻¹ is slightly higher than the reference,¹⁰ corresponding to a penetration depth of 84 nm.

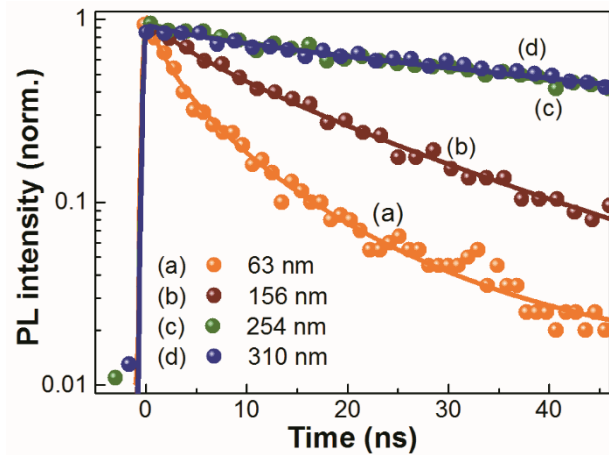


Figure 2. Normalized PL decay curves (circles) of $\text{CH}_3\text{NH}_3\text{PbI}_3$ of different thicknesses ((a) 63 nm, (b) 156 nm, (c) 254 nm and (d) 310 nm, respectively) depending on varied PbI_2 concentration upon excitation at 517 nm, 90 nJ/cm². The solid lines are the stretched exponential fits to the corresponding results.

Table 1. Summary of the stretched exponential fitting for the PL decays in Figure 2.

concentration of PbI_2 (M)	thickness (nm)	τ_s (ns)	β
0.3	63	2.8	0.57
0.5	156	12.6	0.74
0.8	254	90	0.64
1.1	310	91	0.64

The thickness of four prepared perovskite films are determined by a profilometer and listed in Table 1. An insulating polymer poly(methylmethacrylate) (PMMA) layer was coated atop the neat perovskite films for all photoluminescence (PL) decay measurement to passivate their moisture sensitivity.²³ By excitation at 517 nm, their transient fluorescent decay for the peak emission wavelength are shown in Figure 2. The lifetimes for each thickness are also listed in Table 1, fitted by stretch exponential decay function.²⁴ The lifetimes show thickness dependency. For the films of 63 nm and 156 nm, their decays are 2.8 and 12.6 ns, which is similar to the reports.^{10,11} For the two thick films of 254 and 310 nm, they have quite identical fluorescence decay as 90 ns and 91 ns. This means that the fluorescent decay is thickness-dependent in thin film, which disappears in thick ones.

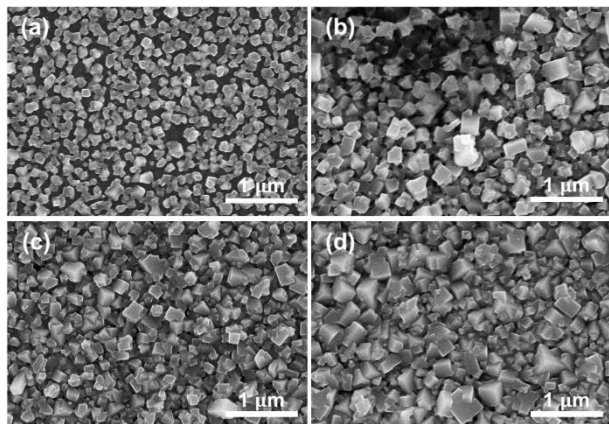


Figure 3. Top-view SEM images of $\text{CH}_3\text{NH}_3\text{PbI}_3$ deposited via changing PbI_2 precursor concentration: (a) 0.3 M; (b) 0.5 M; (c) 0.8 M; and (d) 1.1 M.

The thickness-dependent fluorescence lifetime is analogous to previous reports about perovskite crystal grain size.²⁴ To investigate the influence of crystallite nature on PL properties, a series of scanning electron microscopy (SEM) and X-ray diffraction (XRD) measurement were performed on perovskite films of various PbI_2 concentration (thickness) with no capping layers. Top-view

SEM images of four samples mentioned above are shown in Figure 3a-d. The thinnest film (made by 0.3 M PbI₂) in Figure 3a is a thin layer of individual nanocrystallites with plenty of voids or pinholes. The average grain size is about few tens to ~100 nm. When films became thicker, as shown in Figure 3b-d, the undesirable voids evidently decreased, generating much more compact morphology. Meanwhile, larger crystallites were obtained in thick film, e.g. in Figure 3d, the crystal size is of ~250 nm. This evolution of grain growth is in agreement with previous reported thermally annealed perovskite films.^{12,14} The corresponding XRD patterns (Figure S1 in the SI) clearly show the perovskite structure (14.66 °, 27.09 °, 31.82 °) with the presence of residual unreacted PbI₂, in keeping with a previous study about PbI₂ deposited on flat glasses.²⁰ Moreover, the relative amount of PbI₂ varied, decreasing when thickness increases. Since the fabrication procedures for each sample are the same, this tendency should be attributed to the thickness for different samples.

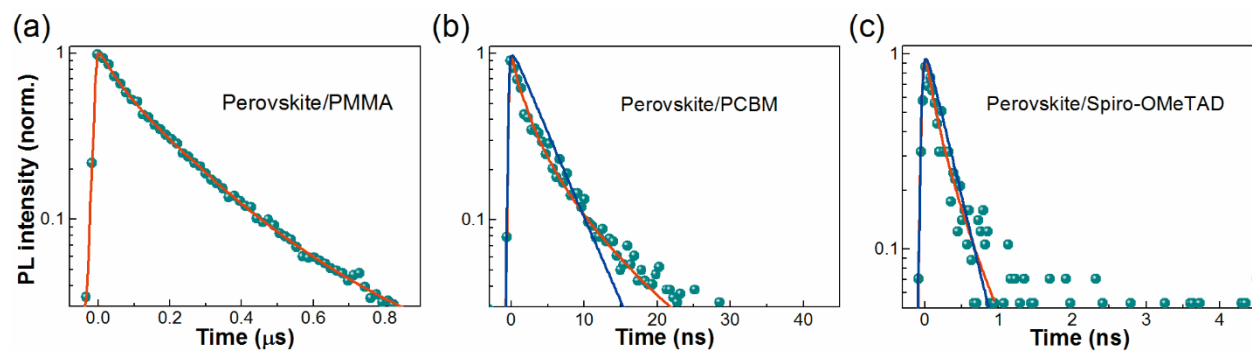


Figure 4. Time-resolved PL decays (dark cyan circles) of (a) spin-coated CH₃NH₃PbI₃ perovskite film (390 nm); (b) film covered by PCBM; and (c) covered by Spiro-OMeTAD, excited at 517 nm. The red and blue solid lines are the fits to the PL results by stretched exponential decay function and one-dimensional diffusion model, respectively.

Table 2. Summary of the fluorescent decay, diffusion coefficients (D), and diffusion lengths (L_D) of a thin and a thick $\text{CH}_3\text{NH}_3\text{PbI}_3$ perovskite films.

thickness (nm)	capping layer	τ_s (ns)	β	D ($\text{cm}^2 \text{s}^{-1}$)	L_D (μm)
~95	PMMA	14.5	0.73	-	-
	PCBM	0.40	0.63	0.045	0.26
	Spiro- OMeTAD	0.16	0.86	0.18	0.51
~390	PMMA	117	0.72	-	-
	PCBM	1.24	0.49	0.14	1.3
	Spiro- OMeTAD	0.17	0.68	2.3	5.2

To examine the charge transfer properties of the $\text{CH}_3\text{NH}_3\text{PbI}_3$ film, transient fluorescence experiments were performed by measuring the PL decay in perovskite film with or without a selected electron or hole acceptor. We made two samples with low and high PbI_2 concentrations, as listed in Table 2. Figure 4 shows the corresponding PL results of a thick perovskite film (390 nm). As shown in Figure 4a and Table 2, the perovskite/PMMA film has a long lifetime of 117 ns, which we will explain in discussion. When the film was coated with a charge transfer layer, PCBM, e.g., fast fluorescent quenching happens (Figure 4b). The decay is as fast as 1.24 ns, which means highly efficient electron transfer to the interface. The hole transfer is even faster, found in Spiro-OMeTAD coated perovskite films, as shown in Figure 4c. The decay is 0.17 ns, close to the instrument response of streak camera. For the thinner film of 95 nm, PL decays show the same trend (Figure S2 in the SI). The neat perovskite film has a lifetime of 14.5 ns, which decreases to 0.40 ns and 0.16 ns for PCBM and Spiro-OMeTAD coated samples, respectively.

The thickness-dependent lifetimes indicate that the fluorescent quenching is nonlocal. This quenching is more like a boundary related effect. Then we suggest that quenching sites are at the grain boundaries. We could propose that the size of the grain become larger when the films are thicker. At same time, the films are more compact with less defects. At certain film thickness, the boundary effect become insignificant. In our study, it is ~ 250 nm, as shown in Figure 2.

The SEM and XRD studies reveal the mechanism of this dependency. The SEM images manifest the evolution of grain growth, from the level of below 100 nm to ~ 250 nm, and the diminishing of voids or pinholes. Ref. 24 claimed that PL lifetime is associated with the grain size. They obtain long lifetime greater than 100 ns in micrometer scale crystallites. We can rationally assume that long lifetime exist when large size of crystallite are the main species in film, and the boundaries between crystallites have a significant impact on the fluorescence characteristic, esp. when the crystal size is small and not so compact. Some groups showed that a proper amount of PbI_2 species can fill perovskite grain boundaries, eliminate defect states, and thus slow down the carrier relaxation, whereas a large amount of excessive PbI_2 is detrimental to charge transport.^{25,26} This is in according with our XRD results for thick and thinner perovskite films, respectively. We believe this is the quenching mechanism of thickness dependent fluorescent lifetime. In short, when the perovskite layer become thicker, it has larger crystallite size with reduce overall grain boundary area, and much less defects due to reduced PbI_2 at boundary. Both the factors finally make the fluorescence emitted from thick film independent to thickness.

It has been well established that excitons in perovskite are nearly fully ionized because of low binding energy.^{2,3,19} So the charge diffusion directly relate to their lifetime. Therefore, the film thickness dependent fluorescent lifetime becomes an important issue here. When the film is thin, the lifetime is short due to the boundary defects. This means that to find out the unaffected charge

diffusion distance, the real lifetime needs to be established in advance. As mentioned earlier, in the thicker film of ~280 nm, a long lifetime of 140 ns can be found at lowest pump intensity.¹⁹ In addition, when the perovskite are in large crystal of ~1 μm , its lifetime is also at ~100 ns timescale.²⁴ These results are very similar to our observation in thick films. It reasonably suggests that the native lifetime for $\text{CH}_3\text{NH}_3\text{PbI}_3$ without considering the boundary defect is at ~100 ns timescale, though small differences exist among research groups. To our knowledge, for reports whose lifetime is ~100 ns, they are all shown as thicker films or larger grain sizes. Therefore, we select thick film of 390 nm for this study.

The one-dimensional diffusion model are describe in the SI. The fittings produce diffusion constant, D . The charge diffusion distance L_D , is calculated by the equation $L_D = \sqrt{D\tau_s}$, where τ_s is PL lifetime of 390 nm in this study. We take the duration when fluorescence decays to 10% of initial intensity as the diffusion time for electrons and holes. As summarized in Table 2, we obtain the electron diffusion coefficient of $0.14 \text{ cm}^2 \text{ s}^{-1}$ and electron diffusion length of ~1.3 μm . This confirms the observation by EBIC method.¹⁶ As a comparing, when we take lifetime of the thinner film, 95 nm, we can calculate the corresponding diffusion constant of $0.045 \text{ cm}^2 \text{ s}^{-1}$ and diffusion length of 256 nm. This result is close to other reports based on thin films.^{10,11,27,28} For diffusion of hole, the D is found $2.3 \text{ cm}^2 \text{ s}^{-1}$ in perovskite/Spiro-OMeTAD film, which is one order larger than the electron diffusion coefficient. The corresponding charge diffusion distance is calculated as ~5.2 μm . For the thin film of 95 nm, this distance is 514 nm, as listed in Table 2. It should be remarked here that both the electron and hole diffusion distance obtained are longer than the thickness of the perovskite film ever made with top solar energy conversion efficiency. This gives a direct support for their high efficiency.

There are several points should be addressed here. The first is that though the charge diffusion distance are thickness dependent, it is larger than the film thickness, even for the thin film less than 100nm. Therefore, even in semi-transparent devices, the high cell performance can also be achieved. The second is that the charge transfer balance between the electrons and holes is not shown in our study. However, it is less important for currently developed devices, which are usually 200-300 nm, since both the carriers can diffuse much longer than the thickness. The last one is that the lifetime of $\text{CH}_3\text{NH}_3\text{PbI}_3$ may not be an exact number but a range around 100ns, since the crystal grain size, defects, preparation procedure, and post treatment et. al. can not exactly be the same. However, the lifetime variation will not make the diffusion distance away from micrometer level. This means the $\text{CH}_3\text{NH}_3\text{PbI}_3$ material has a wide tunable range for its best performance.

In conclusion, we found that the fluorescent lifetime of spin-coated $\text{CH}_3\text{NH}_3\text{PbI}_3$ perovskite thin film depends on the film thickness. The lifetime increases towards the increment of film thickness, till ~ 250 nm. The lifetime finally increases to ~ 100 ns. The fluorescent quenching in thin film is due to the defects at grain boundary. Therefore we take a thick film of 390nm to study the charge diffusion in $\text{CH}_3\text{NH}_3\text{PbI}_3$. After coating charge-transfer layer, PCBM or Spiro-OMeTAD, and applying one-dimensional diffusion model, we can obtain the charge diffusion distance of $1.3 \mu\text{m}$ for electrons and $5.2 \mu\text{m}$ for holes. For thin film of 95nm, a result of short diffusion distance similar to other reports are found. This study resolves the current conflict between the measured short charge diffusion distance and thick working layer in high efficient devices. The result shows that in case of thin and thick films, $\text{CH}_3\text{NH}_3\text{PbI}_3$ both can provide long charge diffusion distance for best cell performance.

ASSOCIATED CONTENT

Supporting Information.

Experimental methods of the fabrication and measurement of the associated perovskite samples investigated in this work. XRD data of perovskite films. PL decays of a thin perovskite (ca. 95 nm) coated with different capping layers. This material is available free of charge via the Internet at <http://pubs.acs.org>.

AUTHOR INFORMATION

Corresponding Author

*Email: wangsf@pku.edu.cn (S.W.); *Email: bianzq@pku.edu.cn (Z.B.).

Author Contributions

[§]Y.L. and W.Y. contributed equally.

Notes

The authors declare no competing financial interests.

ACKNOWLEDGMENT

This work supported by the National Basic Research Program of China 2013CB921904, 2011CB933303; National Natural Science Foundation of China under grant Nos. 11074016, 60878019, 10934001, 61177020, 11134001, 21321001, 21371012.

REFERENCES

- (1) Best Research Cell Efficiency Chart. http://www.nrel.gov/ncpv/images/efficiency_chart.jpg.
- (2) D'Innocenzo, V.; Grancini, G.; Alcocer, M. J.; Kandada, A. R.; Stranks, S. D.; Lee, M. M.; Lanzani, G.; Snaith, H. J.; Petrozza, A. Excitons Versus Free Charges in Organo-Lead Tri-Halide Perovskites. *Nat. Commun.* **2014**, *5*, 3586.
- (3) Sun, S.; Salim, T.; Mathews, N.; Duchamp, M.; Boothroyd, C.; Xing, G.; Sum, T. C.; Lam, Y. M. The Origin of High Efficiency in Low-Temperature Solution-Processable Bilayer Organometal Halide Hybrid Solar Cells. *Energy Environ. Sci.* **2014**, *7*, 399-407.
- (4) Stoumpos, C. C.; Malliakas, C. D.; Kanatzidis, M. G. Semiconducting Tin and Lead Iodide Perovskites with Organic Cations: Phase Transitions, High Mobilities, and near-Infrared Photoluminescent Properties. *Inorg. Chem.* **2013**, *52*, 9019-9038.
- (5) Grätzel, M. The Light and Shade of Perovskite Solar Cells. *Nat. Mater.* **2014**, *13*, 838-842.
- (6) Poncea, C. S.; Savenije, T. J.; Abdellah, M.; Zheng, K.; Yartsev, A.; Pascher, T.; Harlang, T.; Chabera, P.; Pullerits, T.; Stepanov, A. et al. Organometal Halide Perovskite Solar Cell Materials Rationalized: Ultrafast Charge Generation, High and Microsecond-Long Balanced Mobilities, and Slow Recombination. *J. Am. Chem. Soc.* **2014**, *136*, 5189-5192.
- (7) Marchioro, A.; Teuscher, J.; Friedrich, D.; Kunst, M.; van de Krol, R.; Moehl, T.; Grätzel, M.; Moser, J.-E. Unravelling the Mechanism of Photoinduced Charge Transfer Processes in Lead Iodide Perovskite Solar Cells. *Nat. Photon.* **2014**, *8*, 250-255.
- (8) Shen, Q.; Ogomi, Y.; Chang, J.; Tsukamoto, S.; Kukihara, K.; Oshima, T.; Osada, N.; Yoshino, K.; Katayama, K.; Toyoda, T. et al. Charge Transfer and Recombination at the Metal Oxide/CH₃NH₃PbCl₂/spiro-OMeTAD Interfaces: Uncovering the Detailed Mechanism Behind High Efficiency Solar Cells. *Phys. Chem. Chem. Phys.* **2014**, *16*, 19984-19992.

(9) Snaith, H. J. Perovskites: The Emergence of a New Era for Low-Cost, High-Efficiency Solar Cells. *J. Phys. Chem. Lett.* **2013**, *4*, 3623-3630.

(10) Xing, G.; Mathews, N.; Sun, S.; Lim, S. S.; Lam, Y. M.; Grätzel, M.; Mhaisalkar, S.; Sum, T. C. Long-Range Balanced Electron- and Hole-Transport Lengths in Organic-Inorganic $\text{CH}_3\text{NH}_3\text{PbI}_3$. *Science* **2013**, *342*, 344-347.

(11) Stranks, S. D.; Eperon, G. E.; Grancini, G.; Menelaou, C.; Alcocer, M. J.; Leijtens, T.; Herz, L. M.; Petrozza, A.; Snaith, H. J. Electron-Hole Diffusion Lengths Exceeding 1 Micrometer in an Organometal Trihalide Perovskite Absorber. *Science* **2013**, *342*, 341-344.

(12) Liu, D.; Gangishetty, M. K.; Kelly, T. L. Effect of $\text{CH}_3\text{NH}_3\text{PbI}_3$ Thickness on Device Efficiency in Planar Heterojunction Perovskite Solar Cells. *J. Mater. Chem. A* **2014**, *2*, 19873-19881.

(13) Hu, Q.; Wu, J.; Jiang, C.; Liu, T.; Que, X.; Zhu, R.; Gong, Q. Engineering of Electron-Selective Contact for Perovskite Solar Cells with Efficiency Exceeding 15%. *ACS Nano* **2014**, *8*, 10161-10167.

(14) Xiao, Z.; Dong, Q.; Bi, C.; Shao, Y.; Yuan, Y.; Huang, J. Solvent Annealing of Perovskite-Induced Crystal Growth for Photovoltaic-Device Efficiency Enhancement. *Adv. Mater.* **2014**, *26*, 6503-6509.

(15) Gonzalez-Pedro, V.; Juarez-Perez, E. J.; Arsyad, W. S.; Barea, E. M.; Fabregat-Santiago, F.; Mora-Sero, I.; Bisquert, J. General Working Principles of $\text{CH}_3\text{NH}_3\text{PbX}_3$ Perovskite Solar Cells. *Nano Lett.* **2014**, *14*, 888-893.

(16) Edri, E.; Kirmayer, S.; Henning, A.; Mukhopadhyay, S.; Gartsman, K.; Rosenwaks, Y.; Hodes, G.; Cahen, D. Why Lead Methylammonium Tri-Iodide Perovskite-Based Solar Cells Require a Mesoporous Electron Transporting Scaffold (but Not Necessarily a Hole Conductor). *Nano*

Lett. **2014**, *14*, 1000-1004.

(17) Dong, Q.; Fang, Y.; Shao, Y.; Mulligan, P.; Qiu, J.; Cao, L.; Huang, J. Electron-Hole Diffusion Lengths $> 175 \mu\text{m}$ in Solution-Grown $\text{CH}_3\text{NH}_3\text{PbI}_3$ Single Crystals. *Science* **2015**, *347*, 967-970.

(18) Bergmann, V. W.; Weber, S. A.; Javier Ramos, F.; Nazeeruddin, M. K.; Grätzel, M.; Li, D.; Domanski, A. L.; Lieberwirth, I.; Ahmad, S.; Berger, R. Real-Space Observation of Unbalanced Charge Distribution inside a Perovskite-Sensitized Solar Cell. *Nat. Commun.* **2014**, *5*, 5001.

(19) Yamada, Y.; Nakamura, T.; Endo, M.; Wakamiya, A.; Kanemitsu, Y. Photocarrier Recombination Dynamics in Perovskite $\text{CH}_3\text{NH}_3\text{PbI}_3$ for Solar Cell Applications. *J. Am. Chem. Soc.* **2014**, *136*, 11610-11613.

(20) Burschka, J.; Pellet, N.; Moon, S. J.; Humphry-Baker, R.; Gao, P.; Nazeeruddin, M. K.; Grätzel, M. Sequential Deposition as a Route to High-Performance Perovskite-Sensitized Solar Cells. *Nature* **2013**, *499*, 316-319.

(21) Yan, W.; Li, Y.; Li, Y.; Ye, S.; Liu, Z.; Wang, S.; Bian, Z.; Huang, C. Stable and High-Performance Hybrid Perovskite Solar Cells with Ultrathin Polythiophene as Hole-Transporting Layer. *Nano Res.* **2015**, DOI: 10.1007/s12274-015-0755-5.

(22) Park, N.-G. Perovskite Solar Cells: An Emerging Photovoltaic Technology. *Mater. Today* **2015**, *18*, 65-72

(23) Frost, J. M.; Butler, K. T.; Brivio, F.; Hendon, C. H.; van Schilfgaarde, M.; Walsh, A. Atomistic Origins of High-Performance in Hybrid Halide Perovskite Solar Cells. *Nano Lett.* **2014**, *14*, 2584-2590.

(24) D'Innocenzo, V.; Srimath Kandada, A. R.; De Bastiani, M.; Gandini, M.; Petrozza, A. Tuning

the Light Emission Properties by Band Gap Engineering in Hybrid Lead Halide Perovskite. *J. Am. Chem. Soc.* **2014**, *136*, 17730-17733.

(25) Chen, Q.; Zhou, H.; Song, T. B.; Luo, S.; Hong, Z.; Duan, H. S.; Dou, L.; Liu, Y.; Yang, Y. Controllable Self-Induced Passivation of Hybrid Lead Iodide Perovskites toward High Performance Solar Cells. *Nano Lett.* **2014**, *14*, 4158-4163.

(26) Wang, L.; McCleese, C.; Kovalsky, A.; Zhao, Y.; Burda, C. Femtosecond Time-Resolved Transient Absorption Spectroscopy of CH₃NH₃PbI₃ Perovskite Films: Evidence for Passivation Effect of PbI₂. *J. Am. Chem. Soc.* **2014**, *136*, 12205-12208.

(27) Docampo, P.; Hanusch, F. C.; Stranks, S. D.; Döblinger, M.; Feckl, J. M.; Ehrensparger, M.; Minar, N. K.; Johnston, M. B.; Snaith, H. J.; Bein, T. Solution Deposition-Conversion for Planar Heterojunction Mixed Halide Perovskite Solar Cells. *Adv. Energy Mater.* **2014**, *4*, 1400355.

(28) Xie, F. X.; Zhang, D.; Su, H.; Ren, X.; Wong, K. S.; Grätzel, M.; Choy, W. C. H. Vacuum-Assisted Thermal Annealing of CH₃NH₃PbI₃ for Highly Stable and Efficient Perovskite Solar Cells. *ACS Nano* **2014**, *9*, 639-646.

Supporting Information

Direct Observation of Long Electron-Hole Diffusion Distance beyond 1 Micrometer in $\text{CH}_3\text{NH}_3\text{PbI}_3$ Perovskite Thin Film

Yu Li,^{†,a} Weibo Yan,^{†,b} Yunlong Li,^b Wei Wang,^a Zuqiang Bian,^{b,} Lixin Xiao,^a Shufeng Wang,^{a,*} Qihuang Gong^a*

^aInstitute of Modern Optics & State Key Laboratory for Artificial Microstructure and Mesoscopic Physics, School of Physics, Peking University, Beijing 100871, China.

^bState Key Laboratory of Rare Earth Materials Chemistry and Applications, College of Chemistry and Molecular Engineering, Peking University, Beijing, 100871, China

AUTHOR INFORMATION

Corresponding Author

*Email: wangsf@pku.edu.cn; *Email: bianzq@pku.edu.cn.

Experimental Methods

Sample preparation. All samples were fabricated on glass slide substrates. First, glass substrates were cleaned sequentially by ultrasonic bath in detergent water, deionized water, acetone and ethanol for 15 min, respectively, and then exposed to oxygen plasma for 15min to achieve optically smooth films. The $\text{CH}_3\text{NH}_3\text{PbI}_3$ perovskite were fabricated with a two-step sequential deposition method under nitrogen atmosphere. The pre-cleaned glass substrates were spin-coated a PbI_2 solution (6000 rpm, 0.3 M, 0.5 M, 0.8 M, and 1.1 M) of *N,N*-dimethylformamide (DMF) at ambient temperature to obtain layers of different thicknesses. After drying at 60 °C in ambient environment for 6 h, the films were dipped into $\text{CH}_3\text{NH}_3\text{I}$ solution in 2-propanol (10 mg mL^{-1}) at 65 °C for 90 s and then rinsed with 2-propanol. After $\text{CH}_3\text{NH}_3\text{PbI}_3$ annealing at 100 °C for 40 min, Spiro-OMeTAD (10 mg mL^{-1}), PCBM (10 mg mL^{-1}) or PMMA (20 mg mL^{-1}) was spin-coated at 2000 rpm for 60 s atop the $\text{CH}_3\text{NH}_3\text{PbI}_3$ perovskite films.

Characterization Details. X-ray diffraction (XRD) patterns were obtained using a Philips X'PERT-MRD x-ray diffractometer system with a $\text{Cu K}\alpha$ radiation source ($\lambda=0.1541 \text{ nm}$) at 45 kV and 40 mA. Scanning electron microscope (SEM) images were collected using a Hitachi S-4800 microscope, with a working bias of 10 KV. Sample thicknesses were measured using a Veeco Dektak 150 profilometer. Ultraviolet-visible (UV-vis) absorption measurements were recorded with an Agilent 8453 UV-vis Spectroscopy System at room temperature. The absorption (A) was calculated using:

$$A = -\log\left(\frac{I_s}{I_0}\right)$$

(S1)

where I_s is the reference intensity measured with the blank and I_0 is the intensity measured with the sample.

The absorption coefficient α was obtained from:

$$T = \frac{I_s}{I_0} = \exp(-\alpha L)$$

(S2)

where T represents transmittance and L is the sample thickness.

From Equation S1 and S2, we can get the absorption coefficient by the value of A :

$$\alpha = A \cdot \ln 10 / L$$

(S3)

The absorption coefficient for $\text{CH}_3\text{NH}_3\text{PbI}_3$ is as a function of wavelength. The penetration depth $\tau(\lambda)$ is then calculated as $\tau(\lambda) = 1/\alpha(\lambda)$.

The time-resolved fluorescence spectra were recorded with a high resolution streak camera system (Hamamatsu C10910). We used an amplified mode-lock Ti: Sapphire femtosecond laser system (Legend, Coherent) and a two-stage optical parametric amplifier (Opera Solo, Coherent) to generate the pump beam with a repetition rate of 1 KHz. All the samples were excited by 517nm at room temperature with a fluence of $\sim 90 \text{ nJ cm}^{-2}/\text{pulse}$.

Calculation of charge diffusion coefficient and diffusion length.

The charge diffusion length was calculated based on one-dimensional diffusion model which was described in Xing's paper (Ref. 10 in main text) as below:

$$N(t) = \frac{2n_0L}{\pi} \exp(-k(t)t) \sum_{m=0}^{\infty} \left(\exp\left(-\frac{\pi^2 D}{L^2} \left(m + \frac{1}{2}\right)^2 t\right) \frac{\exp(-\alpha L) \pi \left(m + \frac{1}{2}\right) + (-1)^m \alpha L}{\left((\alpha L)^2 + \pi^2 \left(m + \frac{1}{2}\right)^2\right) \left(m + \frac{1}{2}\right)} \right)$$

(S4)

where $N(t)$ is overall photocarrier density within perovskite film, D is the diffusion coefficient, n_0 is initial photoinduced carrier distribution, $k(t)$ is the observed PL decay rate without any quencher layers, α is the absorption coefficient, and L is the thickness of perovskite layer.

By fitting time-resolved PL results we can obtain the expression of $k(t)$. All PL decay curves in our experiments are fitted by stretched exponential model using a professional software (FluoFit, PicoQuant GmbH):

$$I(t) = I_0 e^{-(t/\tau_s)^\beta}$$

(S5)

From Equation (S5) we can obtain the expression of $k(t) = \beta \tau_s^{-\beta} t^{\beta-1}$. Sequentially $N(t)$ is used to fit the PL decay of perovskite films coated with quenchers to derive the value of D . It is notable that the observed PL intensity $I(t)$ is the convolution of the intrinsic PL intensity $f(t)$ and the instrument response function (IRF) $g(t)$:

$$I(t) = \int g(t-t') f(t-t') dt'$$

(S6)

So by fitting the observed PL decay with the convolution of $N(t)$ and IRF gives the estimated D value. Finally the charge carrier diffusion length L_D is calculated by $L_D = \sqrt{D\tau_s}$, where τ_s is the fitted PL lifetime in the case of no quenching layers.

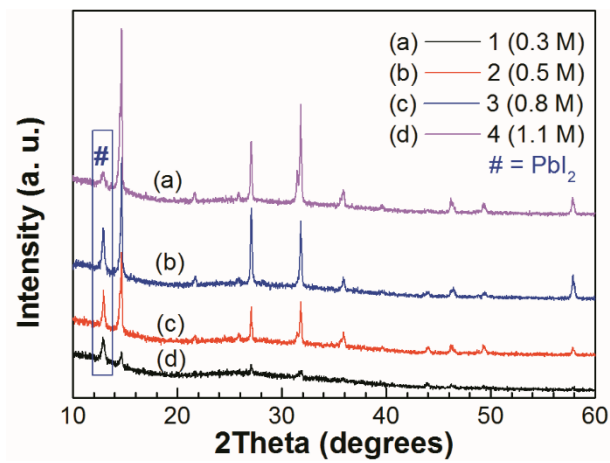


Figure S1. XRD patterns of $\text{CH}_3\text{NH}_3\text{PbI}_3$ films fabricated with varied PbI_2 concentration: (a) 0.3 M, (b) 0.5 M, (c) 0.8 M, and (d) 1.1 M.

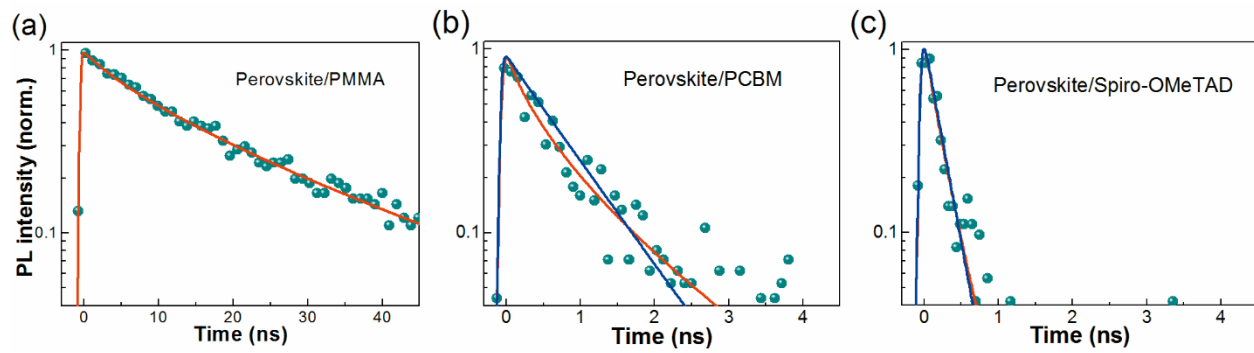


Figure S2. PL decays (dark cyan circles) of $\text{CH}_3\text{NH}_3\text{PbI}_3$ perovskite (ca. 95 nm) coated with (a) PMMA, (b) PCBM and (c) Spiro-OMeTAD layer, taken at the peak emission wavelength, excited at 517 nm. The red and blue solid lines are the fits to the PL results by using stretched exponential function and one-dimensional diffusion model, respectively.